Geophys. Astrophys. Fluid Dynamics, Vol. 61, pp. 75–99
Reprints available directly from the publisher
Photocopying permitted by license only

ON THE TOPOGRAPHIC DEPHASING AND AMPLITUDE MODULATION OF NONLINEAR ROSSBY WAVE INTERACTIONS

WARREN C. CREE

Division of Meteorology, Department of Geography, University of Alberta, Edmonton, Alberta T6G 2G1, Canada

GORDON E. SWATERS†

Applied Mathematics Institute, Department of Mathematics, also Institute of Geophysics, Meteorology and Space Physics, University of Alberta, Edmonton, Alberta T6G 2G1, Canada

(*Received 6 February 1991; in final form 21 May 1991*)

A theoretical study is presented describing large-scale topographic dephasing and amplitude modulation of Rossby wave triads. The model equations are derived via a multiple-scale asymptotic expansion in which it is assumed that topographic gradients vary over a length-scale comparable to the length-scale over which the nonlinear interactions make an order-one contribution to the dynamics. The wave-wave interactions conserve both energy and enstrophy, and preserve the Manley-Rowe relations. It is shown that, in the presence of topographic forcing, the nonlinear energy exchange will induce a permanent wavenumber mismatch in the sense that the wave resonance conditions are no longer completely satisfied. The detuning of the wave triad results in a significant reduction in the energy transfer between the individual waves. The magnitude of the wavenumber mismatch is shown to be dependent on the initial envelope amplitudes, the magnitude of the topographic slope parameter and the underlying carrier wave frequencies and wavenumbers. Even after a triad has traversed a topographic feature of finite zonal extent, it is shown that the energy exchange remains permanently suppressed but is not completely eliminated. Also, the wavelength associated with the energy exchange cycle is shown to be permanently reduced. For several simple topographic configurations exact solutions of the nonlinear steady-state and time-dependent interaction equations can be obtained. In particular a detailed description of the nonlinear interaction characteristics of a Rossby triad over a simple but illustrative triangular topographic feature of finite zonal extent is given.

KEY WORDS: Wave-wave interactions, nonlinear waves, solitons, solitary waves, Rossby waves, planetary waves.

1. INTRODUCTION

The interactions between planetary-scale Rossby waves, by which the velocity field of one wave advects the vorticity field of another wave, and can lead to an amplitude coupling and energy transfer between an ensemble of waves (for example, Longuett-Higgins and Gill, 1967; Phillips, 1981; Pedlosky, Sec. 3.26, 1987), have been proposed as prototypical mechanisms for the onset of anomalous atmospheric

† Corresponding Author.

circulation patterns such as regional blocking or sudden stratospheric warmings (for example, Egger, 1978; Tung and Lindzen, 1979a, b). In the oceanographic context, Hsieh and Mysak (1980) showed that there was observational evidence for resonant shelf wave interactions on the Oregon shelf, and Galvin (1965) and Guza and Inman (1975) provided evidence for resonant edge waves on beaches. There is also the now classic work by Phillips (1960, 1961) describing resonant interactions between quartets of surface gravity waves.

However, many of these earlier studies, notwithstanding their importance, have generally focussed on the *unforced* interactions of resonant wave packets, or have neglected to account for truly nonlinear interactions between the waves, if the ensemble is forced. The study of the nonlinear interactions in a resonant Rossby wave triad under the influence of some type of external forcing, e.g., thermal or topographic, has yet to be undertaken. Presumably, if wave-wave energy exchange plays a role in the formation, maintenance and breakdown of anomalous circulation patterns in geophysical fluids, then external influences are likely to be important in partially explaining the preferred geographical location of the rapid amplification of these wave processes (for example see the study by Warn and Brasnett, 1983). The principal purpose of this paper is to present a theoretical study of the large-scale orographic modulation of interacting Rossby wave triads.

The outline of this paper is as follows. In Section 2 the topographically-forced interaction equations are derived. In order to reduce the dynamics to its simplest form, the basic model we work with is the reduced-gravity potential vorticity equation on an infinite β-plane including the effects of variable topography. The wave-wave interaction equations are derived using a formal multiple-scale asymptotic expansion in which the topography is assumed to vary over the same (long) length-scale as that for which the energy exchange occurs. The topographic feature is assumed to be independent of the meridional coordinate. This is not a crucial simplification in a general sense and it will be obvious how to apply our results to more general orographic configurations. However, in the general development of the theory presented here, the *zonal* form of the topography will be left completely arbitrary. Eventually, we will specialize the topography in order to obtain exact nonlinear solutions to the forced wave-wave interaction equations.

In Section 3 several general properties of the interaction equations are described. In Section 3.1 we briefly summarize some of the most important general results of the three-wave interaction equations needed for our study. In particular, the orographically-forced three-wave interaction equations will conserve both energy and enstrophy and also preserve the appropriate Manley-Rowe relations. In Section 3.2, some simple topographic configurations are presented for which exact *time-dependent* solutions can be obtained for both the fully nonlinear interaction equations and for the approximate "pump-wave" interaction equations. These transformations are very useful in solving the Cauchy or initial-value problem for initial wave packets of finite horizontal extent; for example, triad solitons. In Section 3.3 the details of the exact nonlinear solution to the steady-state equations forced by constant slope topography is presented. In Section 3.4 we show how to patch together solutions of the form obtained in Section 3.3 to describe finite-amplitude wave-wave interactions and transmission over simple topographic features of finite zonal extent.

In Section 4 an example calculation is presented describing the interaction characteristics of a triad over a very simple triangular topographic configuration. Although this orographic shape is very crude, it does serve to illustrate rather nicely the main conclusions that we can infer from our theoretical model. In particular, we will show that in the presence of topographic forcing, the nonlinear energy exchange between the members of the triad will induce a dephasing or wavenumber mismatch. The result of this mismatch can be interpreted as implying that the zonal wavenumber resonance conditions are no longer completely satisfied in a WKB sense and this in turn leads to an inefficient energy transfer between the waves. The precise magnitude of the dephasing parameter is a function of the initial envelope amplitudes, the value of the topographic slope parameter, and the underlying carrier wave frequencies and wavenumbers. As the topographic slope parameter increases, it is shown that the energy transfer between the waves, immediately over the topographic feature, is almost completely eliminated. Moreover, we will show that even after a triad has traversed (i.e., in the sense that a ray path is being followed) a topographic feature of finite horizontal extent, the energy exchange remains permanently suppressed. However, there is some recovery in the efficiency of the wave-wave interaction in the post-topographic region. It is tempting to speculate that the permanence of the dephasing may partly account for why there have been so few observations of resonantly interacting waves in geophysical fluids. In any real atmospheric or oceanic flow there are always many sources of vortex-tube stretching or compression and these influences will almost certainly lead to the dephasing of the resonance conditions. In Section 5 we summarize our work and point out some shortcomings and possible future directions.

2. DERIVATION OF THE INTERACTION EQUATIONS

The derivation of the triad interaction equations when no forcing is present using the method of multiple scales is well known (see, for example, Newell, 1969; Pedlosky, Sec. 3.26, 1987) and thus our presentation will be relatively brief. In order to focus directly on topographically-modulated nonlinear wave-wave interactions, we will work with the relatively simple dynamics described by the equivalent-barotropic potential vorticity equation on a β-plane including the effects of variable orography.

We may write the inviscid nondimensional vorticity equation in the form

$$[\partial_t - \varphi_y \partial_x + \varphi_x \partial_y][\Delta\varphi - \varphi + y + \eta_B] = 0, \tag{2.1}$$

where φ is the geostrophic pressure, $\eta_B(x, y)$ is the bottom topography, x and y are, respectively, the zonal and meridional coordinates and $\Delta = \partial_{xx} + \partial_{yy}$. Subscripts with respect to x, y or t indicate partial differentiation. Although we will focus attention here on inviscid interactions only, Cree (1990) has shown how to include Ekman friction in the derivation of the forthcoming wave-wave interaction equations.

The quasi-geostrophic potential vorticity is given by $\Delta\varphi - \varphi + y + \eta_B$ where each individual term corresponds to the contribution by the relative vorticity, the vorticity associated with the deforming free-surface, the beta-effect, and the vortex-tube

compression associated with the variable topography, respectively. The horizontal length, time and velocity scalings adopted for the above model correspond to $L=R_*$, $T=\beta/R_*$, $U=\beta R_*^2$, respectively, where R_* is the Rossby deformation radius and β is the dimensional beta parameter. The dynamic pressure is scaled geostrophically, i.e., $p^*=f_0 U l \rho$ where f_0 and ρ are, respectively, the constant Coriolis parameter and the constant fluid density. For a complete account of the derivation of the above model see, for example, Pedlosky (1987).

In this paper we want to focus attention directly on what happens to interacting Rossby wave packets as they encounter a meridionally aligned topographic configuration which has a zonal length scale long compared the underlying carrier wavelengths but comparable to the inverse nondimensional wave envelope amplitudes. Our objective is to derive wave-wave interaction equations in a weakly nonlinear context assuming that the effects of topographically-induced vortex-tube stretching are as important as the nonlinear interactions. Consequently, we formally define the topographic height through the relation

$$\eta_B=\int_0^{\varepsilon x}\gamma(x')dx'. \tag{2.2}$$

Here, the zonal gradient of the topography will be given by $\partial_x\eta_B=\varepsilon\gamma(\varepsilon x)$. The parameter ε may be interpreted as the ratio of the deformation radius [which forms the horizontal length-scale in the derivation of (2.1)] to the *actual* horizontal length scale of the topography. Consequently, the limit $0<\varepsilon\ll 1$ will correspond to orography which varies slowly in comparison to a length-scale defined by the deformation radius.

It is important to emphasise here that this scaling will *not* result in a truly forced Rossby wave problem. As we shall see shortly [i.e. (2.8) and (2.10)], this scaling implicitly assumes that, at leading order, the dynamics will be described by an *unforced linear* Rossby wave equation. Thus the analysis presented here will correspond to a situation in which the orography serves only to modify a pre-existing wave triad. When we speak of a "forced" problem in this paper we mean to imply that we are interested in studying the Rossby wave-wave interaction equations when the effects of variable topography occur in the dynamics on the same space and time scales as the nonlinear energy transfers within a weakly nonlinear context.

We will use a multiple-scale procedure to derive the topographically-forced wave-wave interaction equation. Accordingly, we introduce the slow space and time variables

$$\left.\begin{aligned} X&=\varepsilon x,\\ T&=\varepsilon t.\end{aligned}\right\} \tag{2,3a,b}$$

Consequently, (x,t)-derivatives in (2.1) will be rewritten

$$\left.\begin{aligned} \partial_t&\to\partial_t+\varepsilon\partial_T,\\ \partial_x&\to\partial_x+\varepsilon\partial_X.\end{aligned}\right\} \tag{2.4a,b}$$

In order to examine weakly nonlinear dynamics, the geostrophic pressure is rescaled as

$$\varphi(x,y,t)=\varepsilon\tilde{\varphi}(x,y,t;X,T). \tag{2.5}$$

Substitution of (2.2), (2.3), (2.4) and (2.5) into (2.1) yields (after dropping the tilde)

$$(\Delta-1)\varphi_t+\varphi_x=-\varepsilon J(\varphi,\Delta\varphi)-\varepsilon(\Delta-1)\varphi_T-2\varepsilon\varphi_{tX}+\varepsilon\gamma(X)\varphi_y+O(\varepsilon^2), \tag{2.6}$$

where terms of $O(\varepsilon^2)$ have been neglected, and where $J(A,B)=A_xB_y-B_xA_y$.

The solution to (2.6) is obtained in a straightforward asymptotic expansion of the form

$$\varphi\simeq\varphi^{(0)}(x,y,t;X,T)+\varepsilon\varphi^{(1)}(x,y,t;X,T)+\ldots \tag{2.7}$$

Substitution of (2.7) into (2.6) yields O(1) and $O(\varepsilon)$ problems of the form

$$(\Delta-1)\varphi_t^{(0)}+\varphi_x^{(0)}=0, \tag{2.8a}$$

$$(\Delta-1)\varphi_t^{(1)}+\varphi_x^{(1)}=-J(\varphi^{(0)},\Delta\varphi^{(0)})-(\Delta-1)\varphi_T^{(0)}-2\varphi_{tX}^{(0)}-\varphi_X^{(0)}+\gamma(X)\varphi_y^{(0)}, \tag{2.8b}$$

respectively.

The O(1) equations, being linear and not including any topographic forcing, permit a solution consisting of the superposition of three Rossby waves in the form

$$\varphi^{(0)}=\sum_{j=1}^{3}A_j(X,T)\exp(i\theta_j)+\text{c.c.}, \tag{2.9}$$

where the amplitudes $A_j(X,T)$ are slowly varying functions of position and time and the fast phases $\theta_j=k_jx+l_jy-\omega_jt$, $i^2=-1$ and c.c. denotes complex conjugate. Substitution of (2.9) into (2.8a) yields the local dispersion relation

$$\omega_j(k_j^2+l_j^2+1)=-k_j, \tag{2.10}$$

where j is cycled over (1, 2, 3). We shall assume that the three waves in (2.9) form a resonant triad satisfying the well known resonance conditions (without loss of generality)

$$\left.\begin{aligned} k_1+k_2+k_3&=0,\\ l_1+l_2+l_3&=0,\\ \omega_1(k_1,l_1)+\omega_2(k_2,l_2)+\omega_3(k_3,l_3)&=0.\end{aligned}\right\} \tag{2.11a,b,c}$$

The existence of solutions to the dispersion relationship (2.10) which satisfy (2.11) was apparently first pointed out by Kenyon (1964) and later, in greater detail, by Longuet-Higgins and Gill (1967); see also Pedlosky (Sec. 3.26, 1987).

Substitution of (2.9) into the right-hand-side of (2.8b) yields the O(ε) problem in the form

$$(\Delta-1)\varphi_t^{(1)}+\varphi_x^{(1)}=\sum_{j=1}^{3}[(k_j^2+l_j^2+1)A_{jT}-(1+2k_j\omega_j)A_{jx}$$
$$+iA_jl_j\gamma(X)]\exp(i\theta_j)$$
$$+\sum_{n=1}^{3}\sum_{m=1}^{3}A_n^*A_m^*[\hat{\mathbf{e}}_3\cdot(\mathbf{K}_m\times\mathbf{K}_n)(|\mathbf{K}_m|^2-|\mathbf{K}_n|^2)]\exp(-i\theta_n-i\theta_m)$$
$$+\text{other nonresonant terms}+\text{c.c.}, \tag{2.12}$$

where $\mathbf{K}_m=(k_m,l_m)$. The asterisk (*) denotes the complex conjugate. For complete details of the derivation of (2.12) see Cree (1990).

Under the resonance condition (2.11) it follows that the fast phase in the explicitly written out quadratic interaction term in (2.12) has the form $\theta_p=-\theta_n-\theta_m$ where p is that integer from the set $\{1,2,3\}$ different from n and m [i.e., $p=1$ when $n=2$, $m=3$. The case when $n=m$ is not relevant since in this situation the interaction coefficient in (2.12) is identically zero]. The wave-wave interaction equations are obtained from requiring that the coefficients of the complete individual terms proportional to the fast phases θ_1, θ_2 and θ_3 be identically zero. If this demand is not met then is is easy to show that the solution for $\varphi^{(1)}(x,y,t;X,T)$ will necessarily grow linearly with the fast time variable and thus the asymptotic expansion (2.7) will become nonuniform in a time scale of $O(\varepsilon^{-1})$, see Bender and Orszag (1978) or Pedlosky (Sec. 3.26, 1987).

Consequently, in order to preclude the appearance of secular terms in the solution for $\varphi^{(1)}(x,y,t;X,T)$ we require that

$$\left.\begin{aligned}(\partial_T+c_1\partial_X)A_1&=-B_1A_2^*A_3^*-i\mu_1\gamma(X)A_1,\\(\partial_T+c_2\partial_X)A_2&=-B_2A_3^*A_1^*-i\mu_2\gamma(X)A_2,\\(\partial_T+c_3\partial_X)A_3&=-B_3A_1^*A_2^*-i\mu_3\gamma(X)A_3,\end{aligned}\right\} \tag{2.13a,b,c}$$

where

$$\mu_j=l_j/(k_j^2+l_j^2+1), \tag{2.14a}$$

$$c_j=\partial\omega_j/\partial k_j=(k_j^2-l_j^2-1)/(k_j^2+l_j^2+1)^2, \tag{2.14b}$$

$$B_j=[\hat{\mathbf{e}}_3\cdot(\mathbf{K}_n\times\mathbf{K}_m)(|\mathbf{K}_n|^2-|\mathbf{K}_m|^2)]/(k_j^2+l_j^2+1), \tag{2.14c}$$

with (j,n,m) cycled over $(1,2,3)$. Note that c_j is the group velocity associated with the jth wave packet.

For our subsequent discussion it will be convenient to recast the interaction equations (2.13) into "standard" form. To this end we define the new amplitude

functions $\alpha_j(X, T)$ given by

$$\alpha_j(X, T) = A_j(X, T) \exp[i\mu_j \eta_B(X)/c_j], \tag{2.15}$$

for $j = 1, 2, 3$. Substitution of (2.15) into (2.13) yields the interaction equations in the form

$$\left.\begin{aligned}(\partial_T + c_1\partial_X)\alpha_1 &= -B_1\alpha_2^*\alpha_3^* \exp[i\mu_0\eta_B(X)],\\ (\partial_T + c_2\partial_X)\alpha_2 &= -B_2\alpha_1^*\alpha_3^* \exp[i\mu_0\eta_B(X)],\\ (\partial_T + c_3\partial_T)\alpha_3 &= -B_3\alpha_1^*\alpha_2^* \exp[i\mu_0\eta_B(X)],\end{aligned}\right\} \tag{2.16a,b,c}$$

where $\mu_0 = \mu_1/c_1 + \mu_2/c_2 + \mu_3/c_3$.

3. SOLUTIONS OF THE INTERACTION EQUATIONS

3.1 Some General Remarks

It is easy to show that the model (2.16) implies energy and enstrophy conservation, and that the Manley-Rowe relations (Craik, 1985) are also maintained [see (3.19)]. Moreover, it immediately follows from energy conservation, that two of the M_j's in (2.16) are of one sign and the other is of a different sign. It is known (Craik, 1985) that in this situation, the solution to the general initial-value problem for (2.16) will therefore uniquely exist and is, in particular, bounded for all time, at least for sufficiently smooth $\eta_B(X)$. If the interaction coefficients are of the same sign, then at least in the limit $\eta_B \equiv 0$, the solution to the general initial-value problem becomes singular in finite time. This latter situation can occur in weakly nonlinear baroclinic instability (Meacham, 1988).

For a *general* topographic function $\eta_B(X)$, there are no exact solutions as far as we know to either the steady-state or time-dependent interaction equations (2.16). In the absence of topography (i.e., $\eta_B = 0$), the solution to the Cauchy problem for the three-wave interaction equations may be obtained by an Inverse Scattering Transform (*IST*); see Kaup *et al.* (1979) or Craik (1985). If only time or space dependence is retained, then in the limit $\eta_B = 0$, the solutions to the interaction equations may expressed in terms of Jacobi elliptic functions (Bretherton, 1964). In Sections 3.3 and 3.4 we show how to generalize Bretherton's solution to include the effects of variable topography for the simple configuration in which $\eta_B(X)$ is a piece-wise linear continuous function of finite horizontal extent.

3.2 Some Simple Topographic configurations for which Exact Time-Dependent Solutions can be Obtained

There are some special topographic configurations for which, in principle, the *Time-dependent* conservative interaction equations can be solved exactly, i.e., reduced to "canonical" form. Consider the case where $\eta_B(X) = \sigma(X - X_0)^2$, i.e., a parabolic

orographic feature centered at $X = X_0$ with constant curvature (σ is a constant). By introducing the transformations (Riemann *et al.*, 1977)

$$\alpha_j(X, T) = \hat{\alpha}_j(X, T) \exp[i\mu_0 \sigma \hat{\theta}_j (X - X_0 - c_j T)^2], \tag{3.1}$$

where $j = 1, 2$, and 3, and where the $\hat{\theta}_j$ coefficients are given by

$$\hat{\theta}_1 = -c_2 c_3 [(c_2 - c_1)(c_1 - c_3)]^{-1}, \tag{3.2a}$$

$$\hat{\theta}_2 = -c_3 c_1 [(c_3 - c_3)(c_2 - c_1)]^{-1}, \tag{3.2b}$$

$$\hat{\theta}_3 = -c_1 c_2 [(c_1 - c_3)(c_3 - c_2)]^{-1}. \tag{3.2c}$$

into (2.16), one obtains

$$\left.\begin{aligned} (\partial_T + c_1 \partial_X)\hat{\alpha}_1 &= -B_1 \hat{\alpha}_2^* \hat{\alpha}_3^*, \\ (\partial_T + c_2 \partial_X)\hat{\alpha}_2 &= -B_2 \hat{\alpha}_1^* \hat{\alpha}_3^*, \\ (\partial_T + c_3 \partial_X)\hat{\alpha}_3 &= -B_3 \hat{\alpha}_1^* \hat{\alpha}_2^*. \end{aligned}\right\} \tag{3.3a,b,c}$$

The interaction equations (3.3) are exactly of the form (2.16) with no topography present. Since, in principle, the solution to the Cauchy problem associated with (3.3) can be obtained using *IST*, it follows that the time evolution of a Rossby triad forced by a simple parabolic topographic configuration can be determined exactly.

The "pump-wave" approximation to the three-wave interaction equation is a frequently adopted *ansatz* (see, for example, Pedlosky, Sec. 3.26, 1987) wherein one of the three amplitude functions in the wave triad is assumed to be large and constant relative to the other two. Consequently, the dynamics for the two remaining smaller wave amplitudes is linear. For example, if we assume $\alpha_1^*, \alpha_2^* \ll \alpha_3^* \simeq \alpha_{30}^*$ where α_{30}^* is relatively constant, then to leading order, (2.16) educes to the pair of equations.

$$\left.\begin{aligned} (\partial_T + c_1 \partial_X)\alpha_1 &= -B_1 \alpha_2^* \alpha_{30}^* \exp[i\mu_0 \eta_B(X)], \\ (\partial_T + c_2 \partial_X)\alpha_2 &= -B_2 \alpha_1^* \alpha_{30}^* \exp[i\mu_0 \eta_B(X)]. \end{aligned}\right\} \tag{3.4a,b}$$

In the absence of topography (i.e., $\eta_B \equiv 0$) these linear equations can always be solved exactly. A transformation similar to (3.2) exists if η_B is a linear function of the form $\eta_B = \sigma(X - X_0)$ where σ is a slope parameter. In this case if we introduce the transformations

$$\alpha_j(X, T) = \hat{\alpha}_j(X, T) \exp[i\hat{\theta}_j \mu_0 \sigma (X - X_0 - c_j T)], \tag{3.5}$$

where $j = 1$ and 2, and where the $\hat{\theta}_j$ coefficients are given by

$$\hat{\theta}_1 = c_2/(c_1 - c_2), \tag{3.6a}$$

$$\hat{\theta}_2 = c_1/(c_2 - c_1), \tag{3.6b}$$

into (3.4a,b), we obtain

$$(\partial_T + c_1\partial_X)\hat{\alpha}_1 = -B_1\hat{\alpha}_2^*\alpha_{30}^*, \tag{3.7a}$$

$$(\partial_T + c_2\partial_X)\hat{\alpha}_2 = -B_2\hat{\alpha}_1^*\alpha_{30}^*, \tag{3.7b}$$

which have exactly the form of (3.4a,b) assuming no topography. Equations (3.7a,b) can always be written in the form (Craik and Adam, 1978)

$$[\partial_\tau^2 - \partial_\chi^2 + \mathrm{sgn}(B_1B_2)]\hat{\alpha}_j = 0, \tag{3.8}$$

for $j=1$ or 2, and where

$$\tau = |\alpha_{30}|\,|B_1B_2|^{1/2}T, \tag{3.9a}$$

$$\chi = 2|\alpha_{30}|\,|B_1B_2|^{1/2}[X-(c_2+c_1)T/2]/(c_2-c_1), \tag{3.9b}$$

and where $\mathrm{sgn}(B_1B_2)=+1$ if $B_1B_2>0$ and $\mathrm{sgn}(B_1B_2)=-1$ if $B_1B_2<0$. When $\mathrm{sgn}(B_1B_2)=+1$, (3.8) is a *Klein-Gordon* equation and the initial-value problem can be solved by Fourier transforms. If $\mathrm{sgn}(B_1B_2)=-1$, then (3.8) is a *Telegraph* equation and the initial-value problem can be solved by Riemann's method.

3.3 Steady Orographically-Modulated Triad Interactions

In this subsection we present the exact *nonlinear* steady-state solution that can be obtained for the wave amplitudes assuming that the topography is a simple linear function of the form

$$\eta_B = \sigma(X - X_s), \tag{3.10}$$

where the slope parameter σ and "shift" parameter X_s are assumed constant. The solution presented here forms the basic "building-block" in our subsequent work. In Section 3.4 we will use the solution obtained here to construct solutions to the steady interaction equations for simple continuous piece-wise linear topographic configurations of finite horizontal extent, i.e., σ takes on piece-wise constant values; see Figure 1.

The linearly sloping bottom model (3.10) can be viewed simply as an O(ε) "tilting"

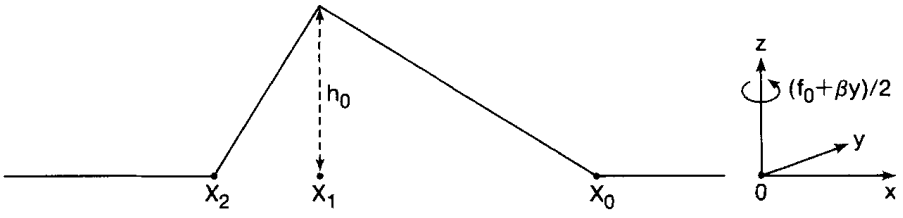

Figure 1 The triangular topographic configuration used to illustrate the theory developed in this paper.

of the β-plane in the governing equations. It is well-known that within the context of the linear O(1) problem (2.8), redefining the effective β will result in an O(ε) correction to the dispersion relationships (2.10). Clearly, if a set of triad wavenumbers and frequencies corresponds to a maximally interacting configuration in the absence of topography it will, in general, no longer be maximally interacting when linear topography is present. The converse is also true of course. However, within the context of the linearly sloping model (3.10), this raises certain problematic aspects with respect to a straightfoward physical interpretation of the solution presented in this section because in any real geophysical fluid there will probably always be triad candidates existing which will be maximally interacting in some regions and not in others should the effective β change for any reason. It is possible that the phase and amplitude variations associated with an initial triad could be lost in any real data set as other triad members become preferred. Nevertheless, all else being equal, if the spectra associated with the maximally interacting triad over a topographic feature was sufficiently different from the unforced maximally interacting triad, one still might be able to extract the evolution of the initial triad from data. It would be interesting to compare the predictions of our theory with the result of numerical simulations.

Substitution of (3.10) into (2.16) and setting the time-derivatives equal to zero, yields

$$\alpha_{1_\xi} = B_{10}\alpha_2^*\alpha_3^* \exp(i\mu_0\sigma\xi), \tag{3.11a}$$

$$\alpha_{2_\xi} = B_{20}\alpha_1^*\alpha_3^* \exp(i\mu_0\sigma\xi), \tag{3.11b}$$

$$\alpha_{3_\xi} = B_{30}\alpha_1^*\alpha_2^* \exp(i\mu_0\sigma\xi), \tag{3.11c}$$

where $B_{j0} = -B_j/c_j$ for $j = 1, 2, 3$ and $\xi = X - X_s$. The solution to (3.11) can be found in the form (Weiland and Wilhelmsson, 1977; Craik, 1985)

$$\alpha_j(\xi) = b_j(\xi)\exp[i\Phi_j(\xi)], \tag{3.12}$$

for $j = 1$, 2 and 3. The $b_j(\xi)$ functions correspond to the envelope amplitudes and the $\Phi_j(\xi)$ will correspond to envelope phase functions. The derivative of Φ_j with respect to x will correspond to a small-amplitude slowly-varying zonal wavenumber correction in the *total* leading-order solution (2.9) which, it will be shown, is induced by the nonlinear wave-wave interactions forced by the variable topography. We shall see momentarily that non-zero Φ_j's lead to a dephasing of the energy exchange.

Substitution of (3.12) into (3.11) leads to, after separating real and imaginary parts,

$$b_{1_\xi} = B_{10}b_2b_3\cos\Phi, \tag{3.13a}$$

$$b_{2_\xi} = B_{20}b_3b_1\cos\Phi, \tag{3.13b}$$

$$b_{3_\xi} = B_{30}b_1b_2\cos\Phi, \tag{3.13c}$$

$$\Phi_{1_\xi} = -B_{10}(b_2b_3/b_1)\sin\Phi, \tag{3.14a}$$

$$\Phi_{2_\xi} = -B_{20}(b_3 b_1/b_2)\sin\Phi, \tag{3.14b}$$

$$\Phi_{3_\xi} = -B_{30}(b_1 b_2/b_3)\sin\Phi, \tag{3.14c}$$

where

$$\Phi(\xi)=\Phi_1(\xi)+\Phi_2(\xi)+\Phi_3(\xi)-\sigma\mu_0\xi. \tag{3.15}$$

Equations (3.14) and (3.15) can be combined to yield

$$\Phi_\xi = -\sigma\mu_0 - b_1 b_2 b_3(B_{10}/b_1^2 + B_{20}/b_2^2 + B_{30}/b_3^2)\sin\Phi. \tag{3.16}$$

Note that the solution for the envelope amplitudes (i.e., b_j's) is obtained from the four equations (3.13) and (3.16), and the envelope phases (i.e., Φ_j's) will be obtained from (3.15) and any two of (3.14).

It is possible to see qualitatively how topography acts to dephase the wave-wave interactions based on (3.13), (3.14) and (3.16). It follows from (3.13) that maximum energy exchange occurs for $\cos(\Phi)=\pm 1$ or equivalently $\Phi=\pm n\pi$ [consequently $\sin\Phi=0$] where n is a nonnegative integer. We may assume, without loss of generality, that initially $\Phi_1=\Phi_2=\Phi_3=0$. In the absence of topography (i.e., $\sigma=0$), it will follow from (3.16) that Φ remains zero thereafter and thus from (3.14) it follows that $\Phi_1=\Phi_1=\Phi_2=0$ for all ξ. In addition, from (3.13) it follows that $\cos\Phi=1$ and hence the energy exchange remains maximized. On the other hand if $\sigma\mu_0\neq 0$ in (3.16), then $\Phi_\xi\neq 0$ initially and the sloping topography will act to induce a nonzero Φ and thus, on account of (3.14), the envelope phases will have magnitudes which will diverge from zero. Also, as Φ moves away from zero, the interaction coefficients in (3.13) will reduce in magnitude and the energy exchange is no longer maximized. We have chosen to call the evolution of the Φ_j's the "dephasing" aspect of the topographically-modified interaction, and the role of Φ in (3.13) the "amplitude modulation" aspect of the interaction.

The solution to (3.13) and (3.16) can be obtained as follows. First, we introduce the renormalizations

$$b_1 = |B_{20}B_{30}|^{-1/2}\hat{b}_1, \tag{3.17a}$$

$$b_2 = |B_{30}B_{10}|^{-1/2}\hat{b}_2, \tag{3.17b}$$

$$b_3 = |B_{10}B_{20}|^{-1/2}\hat{b}_3. \tag{3.17c}$$

Substitution of (3.17) into (3.13) and (3.16) yields

$$\hat{b}_{1_\xi} = s_1\hat{b}_2\hat{b}_3\cos\Phi, \tag{3.18a}$$

$$\hat{b}_{2_\xi} = s_2\hat{b}_3\hat{b}_1\cos\Phi, \tag{3.18b}$$

$$\hat{b}_{3_\xi} = s_3\hat{b}_1\hat{b}_2\cos\Phi, \tag{3.18c}$$

$$\Phi_\xi = -\mu_0\sigma - \hat{b}_1\hat{b}_2\hat{b}_3(s_1/\hat{b}_1^2 + s_2/\hat{b}_2^2 + s_3/\hat{b}_3^2)\sin\Phi, \tag{3.18d}$$

where $s_j = \text{sgn}(B_{j0})$ with $j = 1, 2, 3$. Again, because of energy conservation, it will follow that two of the s_j are of one sign and the other differs in sign. Without loss of generality we can choose $s_2 = s_3 = 1$ and $s_1 = -1$.

If the products $-\hat{b}_1 \times$ (3.18a), $\hat{b}_2 \times$ (3.18b) and $\hat{b}_3 \times$ (3.18c) are formed, it is easy to see that

$$[\hat{b}_1^2(\xi) - \hat{b}_1^2(\xi_0)] = -[\hat{b}_2^2(\xi) - \hat{b}_2^2(\xi_0)] = -[\hat{b}_3^2(\xi) - \hat{b}_3^2(\xi_0)], \tag{3.19}$$

where we have integrated the above products with respect to ξ over the interval (ξ, ξ_0). Equations (3.19) are simply the Manley-Rowe relations for (3.18); see Craik (1985). It will be convenient for our future work to introduce the auxiliary dependent variable

$$\hat{y}(\xi) = -[\hat{b}_1^2(\xi) - \hat{b}_1^2(\xi_0)], \tag{3.20}$$

which on account of (3.19) also satisfies $\hat{y}(\xi) = \hat{b}_j^2(\xi) - \hat{b}_j^2(\xi_0)$ for $j = 1, 2$.

Another auxiliary variable that will be convenient for our subsequent work is the constant of the motion given by

$$\Gamma = \hat{b}_1\hat{b}_2\hat{b}_3\sin\Phi - \mu_0\sigma\hat{b}_1^2/2. \tag{3.21}$$

To show Γ is a constant of the motion it is sufficient to show $\Gamma_\xi = 0$. This can be done by taking the derivative of the left and right-and sides of (3.21) with respect to ξ and eliminating $\hat{b}_{j\xi}$ and Φ_ξ using (3.18).

We are now in a position to derive an ordinary differential equation for $\hat{y}(\xi)$. The solution to $\hat{y}(\xi)$ will be given in terms of elliptic functions. With $\hat{y}(\xi)$ known, the Manley-Rowe relations will determine the $\hat{b}_j(\xi)$ for $j = 1, 2$, and 3. These solutions so obtained will represent orographically-modified triad solutions of the form originally found by, for example, Bretherton (1964).

If we multiply (3.18b) by $\hat{b}_2(\xi)$, it follows that

$$(\hat{b}_2^2)_\xi = \pm\{\hat{b}_1^2\hat{b}_2^2\hat{b}_3^2[1 - \sin^2\Phi]\}^{1/2}. \tag{3.22}$$

Now if (3.20) and the Manley-Rowe relations are used to eliminate the $\hat{b}_j^2$ in (3.22) and (3.21) is used to eliminate $\sin^2\Phi$ in (3.22), it follows that

$$(\hat{y}_\xi)^2 + 2p(\hat{y}) = 0, \tag{3.23a}$$

where $p(\hat{y})$ is given by

$$p(\hat{y}) = [\hat{b}_1^2(\xi_0) - \hat{y}][\hat{b}_2^2(\xi_0) + \hat{y}][\hat{b}_3^2(\xi_0) + \hat{y}] - \{\Gamma - \mu_0\sigma/2[\hat{b}_2^2(\xi_0) + \hat{y}]\}^2. \tag{3.23b}$$

The polynomial $p(\hat{y})$ is cubic in the dependent variable $\hat{y}(\xi)$. It is possible to show

(Wieland and Wilhelmsson, 1977; Craik, 1985) that because not all the s_j coefficients in (3.18) have the same sign (which followed from energy conservation), $p(\hat{y})$ will have three real roots, y_1, $\hat{y}_2$ and $\hat{y}_3$ satisfying $\hat{y}_1 > \hat{y}_2 > \hat{y}_3$. The solution $\hat{y}(\xi)$ will, in general, oscillate between the two largest roots of $p(\hat{y})$. The solution therefore remains bounded. In three-wave interactions where the s_j coefficients are all of the same sign (e.g., Meacham, 1988), it can be shown that the solutions are explosively unstable in that they always become singular at a finite ξ.

The formal solution to (3.23) may be written in the form

$$\xi - \xi_0 = \pm 2^{-1/2} \int_0^{\hat{y}} [-(y-\hat{y}_1)(y-\hat{y}_2)(y-\hat{y}_3)]^{-1/2}\, dy, \tag{3.24}$$

where ξ_0 is a constant of integration for which $y(\xi_0)=0$. Since the roots of $p(\hat{y})$ are all real, the solution may be expressed in the form

$$\hat{y}(\xi) = (\hat{y}_2 - \hat{y}_1)\,\mathrm{sn}^2[(\hat{y}_1 - \hat{y}_3)^{1/2}(\xi - \xi_0) + \hat{\theta}|\hat{k}] + \hat{y}_1, \tag{3.25a}$$

where $\mathrm{sn}(*|*)$ is an elliptic function (Abramowitz and Stegun, 1965) with modulus $\hat{k}$ and shift parameter $\hat{\theta}$ given by,

$$\hat{k} = [(\hat{y}_1 - \hat{y}_2)/(\hat{y}_1 - \hat{y}_3)]^{1/2}, \tag{3.25b}$$

$$\hat{\theta} = \mathrm{sn}^{-1}[\hat{y}_1/(\hat{y}_1 - \hat{y}_2)|\hat{k}]. \tag{3.25c}$$

The "scaled" wavelength of the interaction is given by

$$\lambda_I = \int_0^{2\pi} [1 - \hat{k}\sin^2\Phi]^{-1/2}\, d\xi. \tag{3.26}$$

With the solution for $\hat{y}(\xi)$ given by (3.25), the solution for the amplitudes can be written in the form

$$\hat{b}_1(\xi) = [\hat{b}_1^2(\xi_0) - \hat{y}(\xi)]^{1/2}, \tag{3.27a}$$

$$\hat{b}_2(\xi) = [\hat{b}_2^2(\xi_0) + \hat{y}(\xi)]^{1/2}, \tag{3.27b}$$

$$\hat{b}_3(\xi) = [\hat{b}_3^2(\xi_0) + \hat{y}(\xi)]^{1/2}. \tag{3.27c}$$

The solution for $\Phi(\xi)$ may be obtained by eliminating $\hat{b}_1\hat{b}_2\hat{b}_3\sin(\Phi)$ in (3.18d) using (3.21) and integrating to yield

$$\Phi(\xi) = \Phi(\xi_0) - \mu_0\sigma(\xi - \xi_0) - \int_{\xi_0}^{\xi} [\Gamma + \mu_0\sigma\hat{b}_1^2(\eta)/2][\hat{b}_2^{-2}(\eta) + \hat{b}_3^{-2}(\eta) - \hat{b}_1^{-2}(\eta)]d\eta. \tag{3.28}$$

Similarly, the individual envelope phases may be obtained from (3.14) to yield

$$\Phi_1(\xi)=\Phi_1(\xi_0)+\int_{\xi_0}^{\xi}\hat{b}_2(\eta)\hat{b}_3(\eta)\sin[\Phi(\eta)]/\hat{b}_1(\eta)d\eta, \tag{3.29a}$$

$$\Phi_2(\xi)=\Phi_2(\xi_0)+\int_{\xi_0}^{\xi}\hat{b}_1(\eta)\hat{b}_3(\eta)\sin[\Phi(\eta)]/\hat{b}_2(\eta)d\eta, \tag{3.29b}$$

$$\Phi_3(\xi)=\Phi_3(\xi_0)+\int_{\xi_0}^{\xi}\hat{b}_1(\eta)\hat{b}_2(\eta)\sin[\Phi(\eta)]/\hat{b}_3(\eta)d\eta, \tag{3.29c}$$

3.4 Triad Interactions Over Simple Topographies of Finite Horizontal Extent

The solution presented in Section 3.3 can be used as a building-block to obtain continuous solutions for simple topographic configurations which are continuous and constructed with piece-wise linear sections. Figure 1 illustrates a simple triangular-shaped topographic feature for which such a solution can be obtained. Cree (1990) has described the interaction characteristics for several topographic features of finite extent (for example, ridges) and extended shapes (for example, shelves). Here, we shall only present the solution for the ridge-like feature shown in Figure 1. The topography shown in Figure 1 corresponds to

$$\eta_B(X)=\begin{cases}0, & X<X_2, X\geqslant X_0,\\ h_0(X-X_0)(X_1-X_0)^{-1}, & X_1\leqslant X<X_0,\\ h_0(X-X_2)(X_1-X_2)^{-1}, & X_2\leqslant X<X_1.\end{cases} \tag{3.30a,b,c}$$

The continuous solution for the envelope functions $\alpha_1(X)$, $\alpha_2(X)$ and $\alpha_3(X)$ can be constructed as follows. First, one determines, based on the triad wavenumbers and frequencies, if the energy of the wave packet is travelling eastward (i.e., X increasing) or westward (i.e., X decreasing). Since our solution for the envelope functions is obtained in terms of an initial-value problem in X, if the energy propagates westward, for example, we impose the initial values for the amplitude functions $b_j(X)$ and phase functions $\Phi_j(X)$ in the region $X>X_0$ and compute the B_j's and Φ_j's as X decreases. On the other hand, if the energy propagatin is eastward, then we would impose the initial conditions in the region $X<X_2$ and compute the b_j's and Φ_j's as X increases. In each individual X-interval; $X<X_2$, $X_2\leqslant X<_1$, $X_1\leqslant X<X_0$, and $X\geqslant X_0$ the solution will of the form derived in Section 3.3 for an appropriately determined shift parameter X_s and slope parameter σ in (3.10) in accordance with (3.30). Since, in general, the X_s parameter will be different for the individual regions, the auxiliary independent variable ξ used in the solutions presented in section 3.3 will be different for the individual X-intervals in (3.30). Nevertheless, the solutions for the envelope amplitude and phase functions can be made continuous at the X-interval boundaries (i.e., X_0, X_1 and X_2) by choosing the initial values of the b_j's of the interval just entered, to be the final values of the amplitudes of the region just

exited. One then recomputes the new roots $\hat{y}_1$, $\hat{y}_2$ and $\hat{y}_3$ of the polynomial (3.23b) with the new initial values of the b_j's. The parameter ξ_0 in (3.24) and (3.25a) is then determined so that the *new* $\hat{y}$ satisfies $\hat{y}(\xi_0)=0$ at the X-interval boundary point just passed.

In the numerical example which we will describe in the next Section, the members of the triad will all have negative group velocity and hence westward energy propagation. Consequently, we will now describe the appropriate parameter values to be used, assuming the topographic feature (3.30) is being traversed from right-to-left. For this situation we have

$$\left.\begin{aligned} X_s &= 0, \\ \xi &= X, \\ \sigma &= 0, \\ \xi_0 &= 0, \end{aligned}\right\} \quad \text{in} \quad X \geqslant X_0, \tag{3.31a}$$

$$\left.\begin{aligned} X_s &= X_0, \\ \xi &= X - X_0, \\ \sigma &= h_0/(X_1 - X_0), \\ \xi_0 &= 0, \end{aligned}\right\} \quad \text{in} \quad X_1 \leqslant X < X_0, \tag{3.31b}$$

$$\left.\begin{aligned} X_s &= X_2, \\ \xi &= X - X_2, \\ \sigma &= h_0/(X_1 - X_2), \\ \xi_0 &= X_1 - X_2, \end{aligned}\right\} \quad \text{in} \quad X_2 \leqslant X < X_1, \tag{3.31c}$$

$$\left.\begin{aligned} X_s &= 0, \\ \xi &= X, \\ \sigma &= 0, \\ \xi_0 &= X_2, \end{aligned}\right\} \quad \text{in} \quad X < X_2. \tag{3.31d}$$

It is easy to see how to modify the above procedure to model any number of topographic features provided it can be described by discrete intervals in which the topography has constant slope.

4. AN EXAMPLE CALCULATION

In this section we will present an example calculation for the theory developed in Section 3 for an initially maximally interacting triad composed of Rossby waves with westward-travelling group velocities forced by the simple triangular topographic configuration shown in Figure 1. Cree (1990) has examined the solutions for a variety

of topographic shapes. While the quantitative details of the envelope amplitude and phase depend on the particular topographic configuration, the qualitative details do not and much of what we say can be assumed to apply generally to other topographic shapes.

The wavenumbers and frequencies for the triad used in this example are given approximately by

$$(k_1, l_1, \omega_1) = (-1.08, -1.35, 0.27), \tag{4.1a}$$

$$(k_1, l_2, \omega_2) = (1.00, 1.73, -0.20), \tag{4.1b}$$

$$(k_3, l_3, \omega_3) = (0.08, -0.38, -0.07). \tag{4.1c}$$

The corresponding group velocities are given approximately by

$$c_1 = -0.10, \tag{4.2a}$$

$$c_2 = -0.12, \tag{4.2b}$$

$$c_3 = -0.86. \tag{4.2c}$$

The topographic parameter μ_0 in (2.16) is given approximately by

$$\mu_0 = 0.75, \tag{4.3}$$

and the interaction coefficients in (3.11) are given approximately by

$$B_{10} = -4.8, \tag{4.4a}$$

$$B_{20} = 2.46, \tag{4.4b}$$

$$B_{30} = 0.52. \tag{4.4c}$$

Note that the sign of B_{10} is negative and the signs of B_{20} and B_{30} are positive. We shall, for this example, set

$$X_0 = -10, \tag{4.5a}$$

$$X_1 = -20, \tag{4.5b}$$

$$X_2 = -30. \tag{4.5c}$$

There are resonant triads for which the group velocities are not all of the same sign. These situations all seem to correspond to cases for which the "scaled" interaction coefficients $B_{i0} \equiv -B_i/c_i$, for $i = 1, 2, 3$ in (3.11) all have the same sign (Cree, 1990).

Formally, for these situations, the solutions to (3.11) will always be singular in the sense that there will necessarily exist finite ξ values for which the $\alpha_i(\xi)$ become unbounded. In fact, we would argue that in this situation our "steady-state" theory is no longer valid because if the group velocities are no longer of the same sign the interaction process becomes inherently time-dependent on an O(1) time scale.

The initial values of the envelope amplitudes b_j's and the phase Φ_j's will be specified at the position $X=0$ (see Figure 1). Since we shall assume that initially the resonant triad is maximally interacting, the initial envelope phases will be given by

$$\Phi_1(0)=\Phi_2(0)=\Phi_3(0)=0. \tag{4.6}$$

The wavelength of the wave-wave interaction (i.e., the distance in X over which the energy exchange goes through one complete cycle) is determined in part by the wave amplitudes; see (3.26). For the simulation described here, we have chosen the initial conditions

$$b_1(0)=1.0, \tag{4.7a}$$

$$b_2(0)=0.04, \tag{4.7b}$$

$$b_3(0)=0.02, \tag{4.7c}$$

for amplitudes given in (3.12). These initial values imply that the interaction nondimensional wavelength in the absence of topography is about eleven non-dimension x-units (see Figure 2). This choice is convenient since we will be able to depict the topographically-modified development of the envelope amplitudes and phases through an entire interaction cycle. Cree (1990) has examined the interaction characteristics for a range of initial amplitudes and various topographic shapes and the interested reader is referred there for a more complete description.

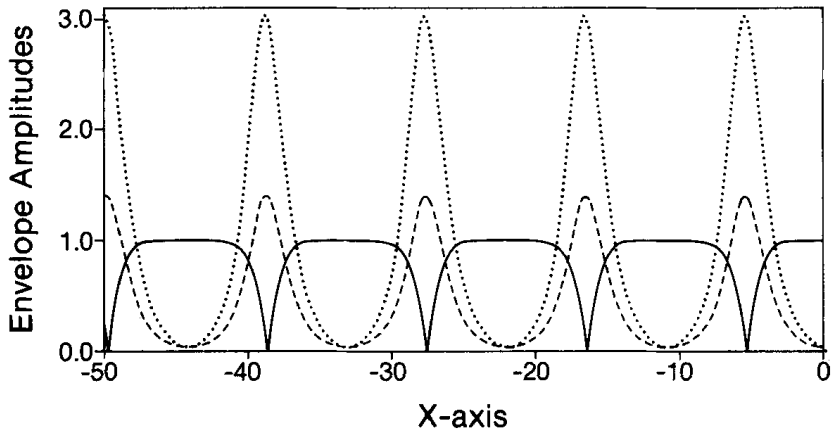

Figure 2 A plot of the wave amplitudes $b_j(X)$ for the initial amplitudes and phases given by (4.7) and (4.6), respectively, assuming *no* topography, i.e., $h_0=0.0$ in (3.30). Wave 1, wave 2 and wave 3 are denoted by the solid, dashed and dotted curves, respectively.

In Figure 2, we show the energy exchange cycle from $X=0.0$ to $X=-50.0$ in the absence of topography (i.e., $h_0=0$). We remind the reader that since the group velocity is negative for all the members of the triad, it may be useful to think of the energy as "starting" at $X=0.0$ and "progressing" to $X=-50.0$ with the relative envelope amplitude magnitudes reflecting the energy partition at a particular moment in time. During the first half of the cycle, for example in the region $-5.5\leqslant X\leqslant 0.0$, we see in Figure 2 that waves 2 and 3 extract energy from wave 1 and during the last half cycle, for example in $-11.0\leqslant X\leqslant -5.5$, energy is transferred back to wave 1 from waves 2 and 3. In the absence of any external forcing this exchange occurs, of course, indefinitely with a fixed spatial/temporal period.

In Figure 3 we show how the energy exchange is modified for a "small" topographic slope parameter of $|\sigma|=1.33$ corresponding to $h_0=13.33$ in (3.30) amd (3.31). In the initial region containing no topography $-10.0<X<0.0$, the energy exchange is unforced and is identical to that depicted in Figure 2. However, over the region of topographic variability $-30.0<X<-10.0$, notice in Figure 3a how the energy partition has been modified. Roughly speaking while energy exchange still occurs, it does so in a less complete fashion in that the magnitude of the amplitude oscillation is reduced. Also, although it is more difficult to see in Figure 3, the effective wavelength over the topography of the interaction has been reduced to about 10.0 nondimensional X-units. Once the topographic feature has been traversed ($X\leqslant -30.0$), The envelope amplitudes appear very similar to their pre-topographic appearance for this small slope value. However, in fact, the oscillation amplitude and interaction length scale have been permanently reduced. These features are more dramatically shown in Figure 4 and 5 where larger slope values have been assumed.

We can see in Figures 3b and 3c how the triad has become "dephased" as a result of topographic forcing. In Figure 3b we plot the phase function $\Phi(X)$ given by (3.15) which appears in the amplitude equations, e.g. (3.13). This function controls the efficiency of the energy exchange. Maximum energy exchange occurs for $\Phi=n\pi$ and minimum exchange occurs for $\Phi=(2n+1)\pi/2$ (n an integer). In the initial no topography region $-10.0<X<0$, we have $\Phi=0$ and hence we have maximum exchange. However, over the region of nonzero topographic slope $-30.0<X<-10.00$, $\Phi(X)$ begins to evolve spatially in accordance with (3.16). Since $\Phi(X)$ begins to diverge from zero over the region of topography variability, the energy exchange is no longer maximal; see (3.13). Moreover, it is important to note from Figure 3b that even *after* the topographic region has been traversed (i.e., the region $X<-30.0$), $\Phi(X)$ is *not* constant (and specifically is not zero) and consequently the wave-wave energy exchange is permanently suppressed. In Figure 3b it appears as if $\Phi(X)$ is relatively constant (and indeed almost zero) in the post-topography region $X<-30.0$ except near $X\simeq -40.0$. The reason why $\Phi(X)$ is relatively constant in this region is because of the relatively small value of h_0 adopted for Figure 3. The sudden increase in the magnitude of h_0 near $X\simeq 40.0$ is due to the fact that the magnitude of the envelope amplitudes $b_2(X)$ and $b_3(X)$ are very small at this point (see Figure 3a) and this, as can be qualitatively inferred from (3.19), will lead to large spatial gradients in $\Phi(X)$. One can see how the magnitude h_0 affects the post-topography variability of the phase function $\Phi(X)$ by comparing Figure 3b with Figures 4b and 5b in which h_0 is given by 40.0 and 66.67, respectively.

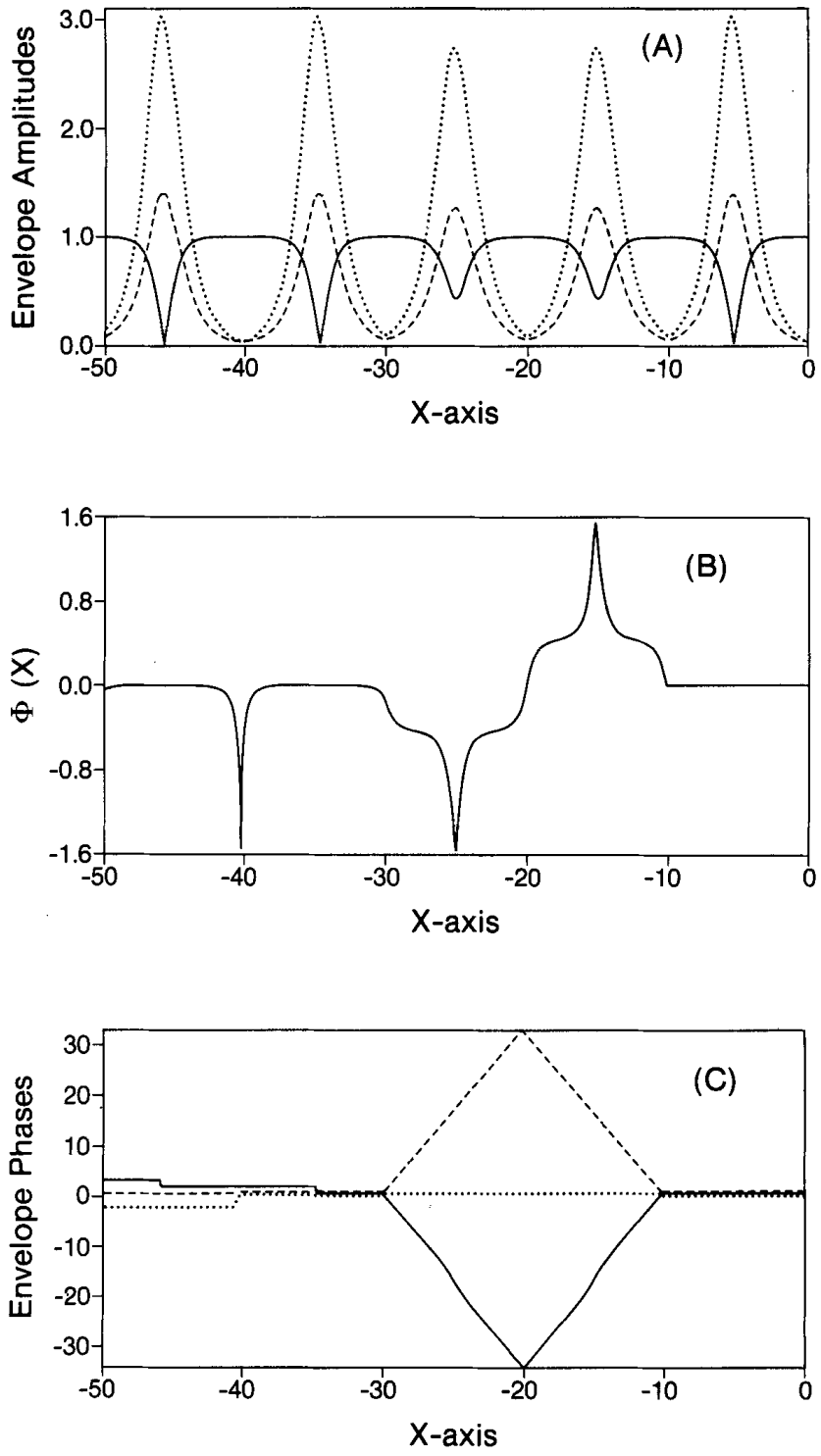

Figure 3 Plots of the envelope amplitudes $b_j(X)$ (Figure 3a), the detuning phase function $\Phi(X)$ (Figure 3b), and the envelope phases $\Phi_j(X)$ (Figure 3c) for a "small" slope value of $|\sigma| = 1.33$. Wave 1, wave 2 and wave 3 are denoted by the solid, dashed and dotted curves, respectively.

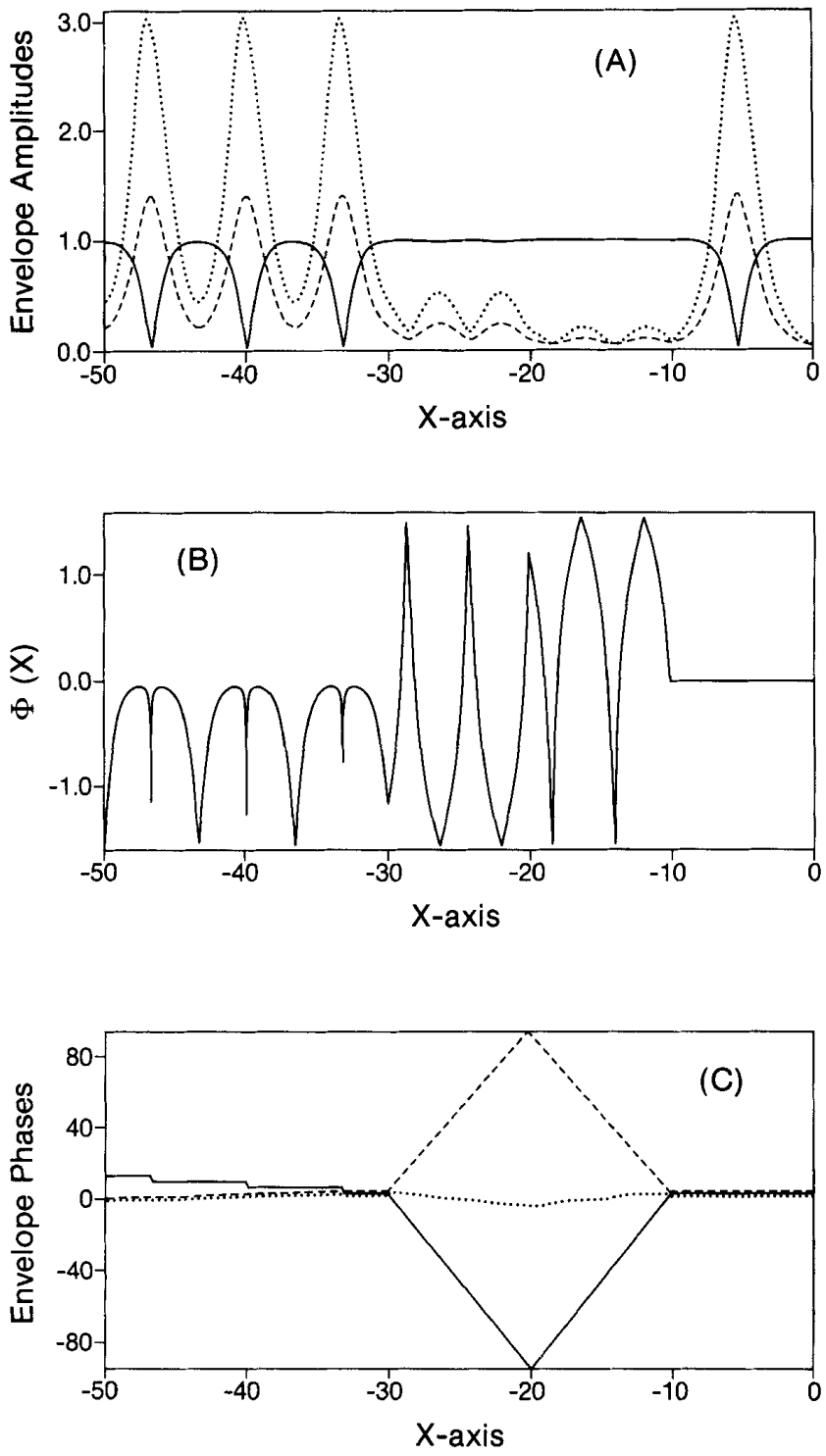

Figure 4 Plots of the envelope amplitudes $b_j(x)$ (Figure 4a), the detuning phase function $\Phi(X)$ (Figure 4b), and the envelope phases $\Phi_j(X)$ (Figure 4c) for a "moderate" slope value of $|\sigma| = 4.0$. Wave 1, wave 2 and wave 3 are denoted by the solid, dashed and dotted curves, respectively.

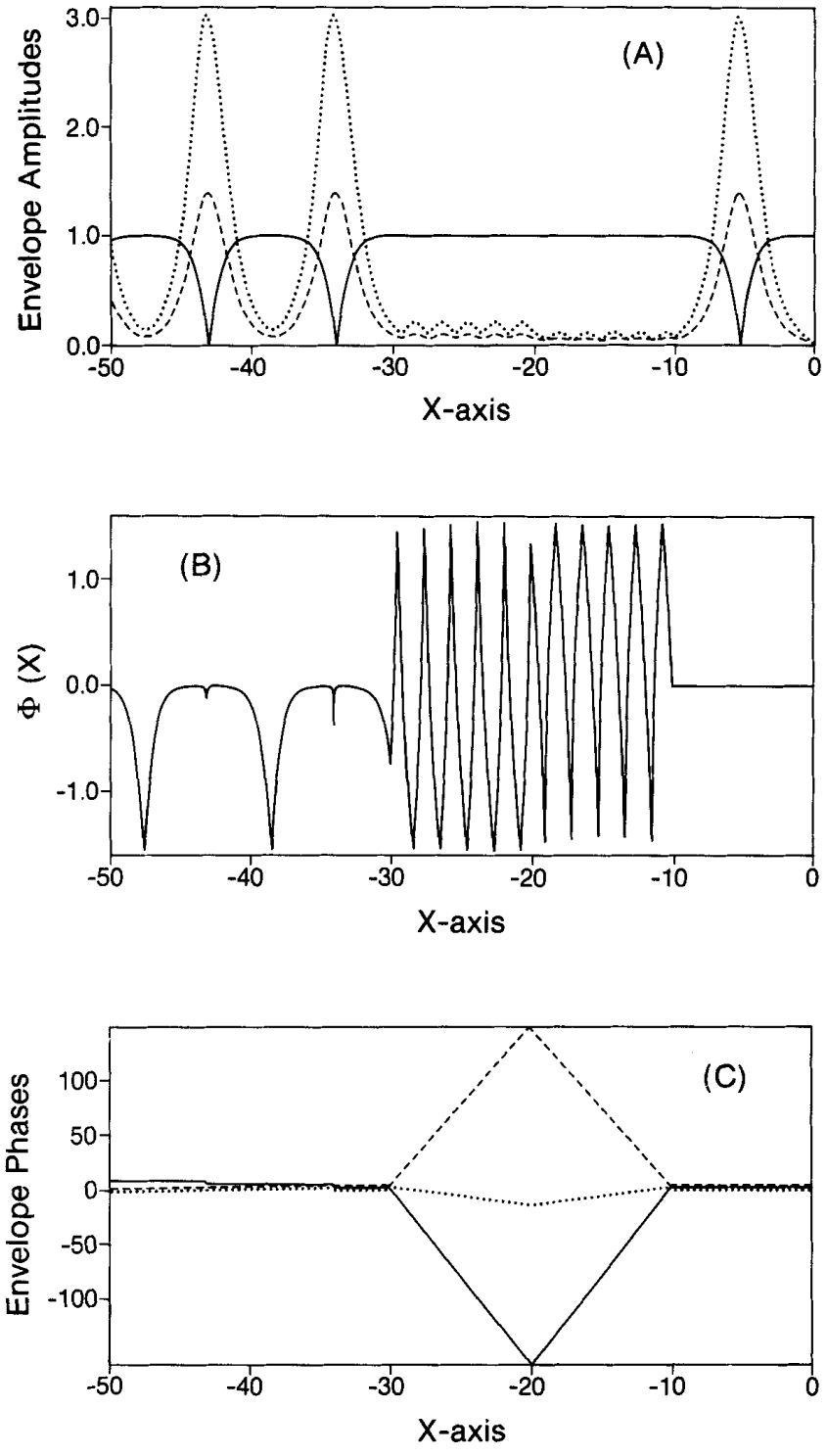

Figure 5 Plots of the envelope amplitudes $b_j(X)$ (Figure 5a), the detuning phase function $\Phi(X)$ (Figure 5b), and the envelope phases $\Phi_j(X)$ (Figure 5c) for a "large" slope value of $|\sigma| = 6.67$. Wave 1, wave 2 and wave 3 are denoted by the solid, dashed and dotted curves, respectively.

In Figure 3c the individual envelope phase functions $\Phi_1(X)$, $\Phi_2(X)$ and $\Phi_3(X)$ are presented as determined by (3.29). We have assumed that $\Phi_j(0)=0$ for $j=1,2,3$. Note that over the topographic region $-30.0\leqslant X\leqslant -10.0$, $\Phi_1(X)$ and $\Phi_2(X)$ experience rapid development compared to $\Phi_3(X)$. This seems to be simply the result of two factors. First, when the integrands in (3.29) are written in terms of the "unscaled" $b_j(X)$ functions given by (3.17), the integrals in (3.29a,b,c) become proportional to $|B_{10}|$, $|B_{20}|$ and $|B_{30}|$, respectively. For the triad (4.1), the value of $|B_{30}|$ given in (4.4) is an order of magnitude less than either $|B_{10}|$ or $|B_{20}|$. This fact coupled with the observation that can be qualitatively made from Figure 3a, that on average b_1b_2/b_3 is less than b_2b_3/b_1 or b_1b_3/b_2, will imply that the contribution from the integrand in (3.29c) will be relatively smaller than the contribution from the integrands in (3.29a) or (3.29b) and, consequently, there is substantially less variability in $\Phi_3(X)$ compared to $\Phi_1(X)$ or Φ_2X) over the topography. Once past the tpopgraphic region, the envelope phases $\Phi_j(X)$ do not have a substantial degree of variability to them, although they are nonzero. Nevertheless because the $\Phi_j(X)$ are nonzero, this will mean that the individual wave packets will be out of phase compared with where they would be in the absence of topography. Again, the fact that the $\Phi_j(X)$ in Figure 3c are relatively constant in the region $X\leqslant -30.0$ is simply the result of the relatively small value of h_o (Compare Figure 3c with Figures 4c and 5c.) Finally, we remark that the locations where $\Phi_1(X)$ and $\Phi_2(X)$ appear to take a "jump" in the post-topography region $X\leqslant -30.0$ correspond to those locations where $b_1(X)$ and $b_2(X)$ have minimum magnitudes, respectively.

In Figures 4 and 5 we show the interaction characteristics for "moderate" and "large" slope parameter values of $|\sigma|=4.0$ and 6.67, respectively. Note how over the topography (i.e., $-30.0\leqslant X\leqslant -10.0$) the energy exchange between the waves has been almost entirely eliminated compared to that shown in Figure 3. Also, one can clearly see in Figures 4a and 5a how the presence of the sloping topography has shortened the interaction wavelength over the topography. There is a slight recovery in the intensity of the energy exchange over the "down-slope" portion of the topography compared to the "up-slope" portion of the topography as manifested by the larger oscillation amplitude in the wave 2 and 3 envelope amplitudes. In the post-topographic region (i.e. $X\leqslant -30.0$), the energy exchange substantially recovers but, nevertheless, the energy exchange is *not* as complete as it was initially. Note how the wave 2 and 3 minimum amplitudes in the post-topographic region are larger than the pre-topographic minimums.

If one compares Figures 4b and 5b with 3b, it is clear that increasing the topographic slope parameter leads to a significant dephasing of the interaction not only over the topographic region, but once past the topography as well. It is the large variability in $\Phi(X)$ for $X\leqslant -30.0$ which leads to a permanent dephasing of the energy exchange. In Figures 4c and 5c we show the individual envelope phases. Here again one can see how increasing the topographic slope parameter leads to significant variability in the envelope phases. (Note that the vertical axes in Figures 3c, 4c and 5c have been scaled differently.)

The fact that $\Phi_X\neq 0$ even in the post-topographic region can be interpreted as saying that the topographically-forced wave-wave interactions induced a permanent

zonal wavenumber mismatch in the trial resonance conditions (2.11). If we backtrack through the transformations (3.17), (3.12), (2.15) and (2.9), it follows that the *total* phase of the jth wave in the triad can be written in the form

$$\psi_j = \theta_j - \mu_j \eta_B(X)/c_j + \Phi_j(X), \tag{4.8}$$

where θ_j is the "fast" phase contribution given by $k_j x + l_j y - \omega_j t$. If we think in terms of a "WKB" *ansatz* we can identify a zonal wavenumber denoted $\kappa_j(\varepsilon x)$, as given by

$$\kappa_j = \partial\psi_j/\partial x = k_j + \varepsilon[(\partial\Phi_j/\partial X) - \mu_j \eta_{B_X}/c_j], \tag{4.9}$$

for $j = 1, 2$, and 3. If the sum $\kappa_1 + \kappa_2 + \kappa_3$ is formed, it follows upon using (2.11) and (3.15) that

$$\sum_{j=1}^{3} \kappa_j = \varepsilon \Phi_X. \tag{4.10}$$

Consequently, if $\Phi_X \neq 0$, it follows that the wave resonance condition on the *complete* WKB zonal wavenumber, including not only the fast phase contribution but also the wave-wave interaction induced contribution, does not hold. We can interpret the $\varepsilon\Phi_X$ term in (4.10) as a zonal wavenumber mismatch.

5. SUMMARY AND DISCUSSION

In this paper we have attempted to develope a theory to describe the topographic modulation of resonantly interacting Rossby waves. In order to focus our attention directly on the wave-wave interaction process, the basic model used was very simple; the equivalent-barotropic potential vorticity equation on an infinite β-plane including bottom topography. The resonant interaction equations were derived using a multiple-scale asymptotic expansion in which it was assumed that horizontal topographic gradients varied over the same length scale as the energy exchange process. This expansion resulted in a set of evolution equations for the wave packet amplitudes including the effects of topography. These forced wave interaction equations retained energy and enstrophy conservation, and also satisfied the Manley-Rowe relations for a resonant triad. Although the main body of this paper was devoted to an analysis of topographically-modulated *steady-state* interactions, in Section 3.1 we included two transformations that can be used to map the *forced* time-dependent wave-wave interaction equations to *unforced* wave-wave interaction equations for special topographic configurations. These transformations will be very useful in developing solutions to the Cauchy problem for topographically-modulated wave-wave interactions.

In Section 3.3 we presented an exact nonlinear solution to the wave-wave interaction equations forced by linearly sloping topography. These solutions are expressed in terms of cnoidal wave functions and are appropriate generalizations of the well known solutions presented in, for example, Bretherton (1964) or Longuett-Higgins and Gill (1967). In Section 3.4, we described how the solutions of

Section 3.3 could be "patched" together in order to obtain an exact solution for wave-wave interactions over simple topographic features of finite horizontal extent. It is important to emphasize again here that the topographic configurations for which we could solve the equations exactly were very specialized in that they were assumed to be continuous piece-wise linear functions of the zonal coordinate. Nevertheless the solutions presented here represent, we believe, the first attempts to provide an analytical description of truly nonlinear energy exchange between topographically-forced Rossby waves. Moreover, in spite of the extreme simplicity of the orography, several interesting features of the modulated interaction have been described.

In particular, we have shown that in the presence of topography the wave-wave interactions induce a dephasing in the sense that the energy exchange is no longer maximal. The dephasing can be interpreted as the development of an oscillatory small-amplitude slow-varying (compared to the underlying carrier phases) zonal wavenumber. The individual envelope topographically-induced phase functions will not, in general, satisfy the triad resonance conditions and this in turn can be interpreted as responsible for the suppression of the energy exchange between the waves. Also, we showed that, to the degree that energy exchange still occurs over the topographic feature, the wavelength or period of the exchange cycle is reduced. Another important conclusion of our study is that even after the wave packets have traversed a topographic feature of finite horizontal extent, the energy exchange remains suppressed. However, the degree to which the waves do not exchange energy depends on the topographic slope and on the initial envelope amplitudes, and underlying carrier wave frequencies and wavelengths. In addition, we found that in the post-topographic region, the wavelength or period of the energy exchange remained permanently decreased.

Although this paper has been directly focussed on orographically-modulated Rossby wave interactions, we believe our general results have application to other examples of wave-wave interactions in geophysical fluids. In particular, if slowly-varying along-shore topographic gradients are retained in shelf or edge wave problems, the resulting interaction equations are presumably of the form (2.13) and thus much of what we have said in this paper is applicable. It may be that much of the geographic localization that Hsieh and Mysak (1980) found in the shelf wave triad interactions observed along Oregon can be attributed to the topographic dephasing and amplitude modulation described here. We believe that this problem deserves further study owing to its oceanographic importance.

There remain several shortcomings to our model. One of the most important is that the interactions that we have examined have been in the main steady. As a result we have not examined in any real detail the initial value problem for topographically-forced interactions of Rossby waves. One interesting problem in this category is the interaction of Rossby packets with finite horizontal extent including variable topography. It is well known that the *unforced* wave-wave interaction equations [i.e. (2.13) with $\gamma(X) \equiv 0$], have soliton solutions. It would be very interesting to develop a theory, similar to those developed by Grimshaw (1979a,b; 1981), for interacting Rossby solitons modulated by topography.

Another problem of interest would be the incorporation of boundary conditions

into the solution. Our underlying physical geometry was an infinite β-plane. Particularly with regard to the atmospheric applicability of our results, it would be interesting to consider developing a theory for a mid-latitude zonal channel with periodic zonal boundary conditions.

Acknowledgements

Preparation of this paper was supported in part by Operating Research Grants awarded by the Natural Sciences and Engineering Research council of Canada, and by Science Subventions awarded by the Atmospheric Environment Service of Canada to G. E. Swaters.

References

Abramowitz, M. and Stegun, J. A., *Handbook of mathematical functions*, Dover (1965).

Bender, C. M. and Orszag, S. A., *Advanced Mathematical Methods for Scientists and Engineers*, McGraw-Hill (1978).

Bretherton, F. P., "Resonant interactions between waves: The case of discrete oscillations," *J. Fluid Mech.* **20,** 457–479 (1964).

Craik, A. D. D., *Wave interactions and fluid flows*, Cambridge university Press (1985).

Craik, A. D. D. and Adam, J. A., "Evolution in space and time of resonant wave triads: I. The "pump-wave approximation," *Proc. R. Soc. Lond.* **A363,** 243-255 (1978).

Cree, W., "Topographic de-phasing and amplitude modulation of Rossby wave triad packets," M.Sc. Thesis, University of Alberta, Edmonton, Canada (1990).

Egger, J., "Dynamics of blocking highs," *J. Atmos. Sci.* **35,** 1788–1801 (1978).

Galvin, C. J., "Resonant edge waves on laboratory beaches," *EOS Trans. AGU* **46,** 122 (1965).

Grimshaw, R. H. J., "Slowly varying solitary waves, I. Korteweg-de Vries equation," *Proc. R. Soc. Lond.* **A368,** 359–375 (1979a).

Grimshaw, R. H. J., "Slowly varying solitary waves, II. Nonlinear Schroedinger equation," *Proc. R. Soc. Lond.* **A368,** 377–388 (1979b).

Grimshaw, R. H. J., "Slowly varying solitary waves in deep fluids," *Proc. R. Soc. Lond.* **A376,** 319–332 (1981).

Guza, R. T. and Inman, D. L., "Edge waves and beach cusps," *J. Geophys. Res.* **80,** 2997–3011 (1975).

Hsieh, W. W. and Mysak, L. A., "Resonant interactions between shelf waves, with applications to the Oregon Shelf," *J. Phys. Oceanogr.* **10**(11), 1729–1741 (1980).

Kaup, D. J., Riemann, A. and Bers, A., "Space-time evolution of nonlinear three-wave interactions: I. Interactions in a homogeneous medium," *Rev. Mod. Phys.* **51,** 275–310 (1979).

Kenyon, K., "Nonlinear Rossby waves," Summer study program in geophysical fluid dynamics. Woods Hole Oceanographic Institution, Volume **2** (1964).

Longuett-Higgins, M. S. and Gill, A. E., "Resonant interactions between planetary waves," *Proc. R. Soc. Lond.* **A229,** 120–140 (1967).

Mecham, S., "Non-modal baroclinic instability," *Dyn. Atmos. Oceans* **12,** 19–45 (1988).

Newell, A. C., "Rossby wave packet interactions," *J. Fluid Mech.* **35**(2), 255–271 (1969).

Pedlosky, J., *Geophysical Fluid Dynamics*, Springer-Verlag (1987).

Phillips, O. M., "On the dynamics of unsteady gravity waves of finite amplitude. Part I," *J. Fluid Mech.* **9,** 193–217 (1960). Part II, ibid. **11,** 143–155 (1961).

Phillips, O. M., "Wave interactions—the evolution of an idea," *J. Fluid Mech.* **106,** 215–227 (1981).

Riemann, A. H., Bers, A. and Kaup, D. J., "Nonlinear interactions of three wave packets in an inhomogeneous medium," *Phys. Rev. Lett.* **39**(5), 245–248 (1977).

Warn, T. and Brasnett, B., "The amplification and capture of atmospheric solitons by topography: A theory of the onset of regional blocking," *J. Atmos. Sci.* **40,** 28–38 (1983).

Weiland, J. and Wilhelmsson, H., *Coherent nonlinear interaction of waves in plasmas*, Pergamon (1977).

Tung, K. K. and Lindzen, R. S., "A theory of stationary long waves: Part I. A simple theory of blocking," *Mon. Wea. Rev.* **107,** 714–734 (1979a).

Tung, K. K. and Lindzen, R. S., "A theory of stationary long waves: Part II. Resonant Rossby waves in the presence of realistic vertical shears," *Mon. Wea. Rev.* **107,** 735–750 (1979b).